Decarburisation rates in RH–KTB degasser of CST steel plant through physical modelling study

V. Seshadri*[1], C. A. da Silva[2], I. A. da Silva[2], G. A. Vargas[3] and P. S. B. Lascosqui[3]

A physical model based on similarity principles was constructed to simulate the RH (Ruhrstahl–Heraeus) degasser of CST (Companhia Siderúrgica Tubarão, Vitória, Brazil) to evaluate the influence of metal circulation rate, which essentially defines the degree of exposure of the metal to the vacuum in the chamber, on the decarburisation rate. The circulation rate in addition influences the removal of dissolved gases such as nitrogen, and hence it is essential to optimise this parameter to achieve maximum refining efficiency with minimum refining time, thus improving the productivity of the secondary refining process. In the present work, simulation experiments investigating the kinetics of decarburisation have been carried out using the CO_2 adsorption–desorption process in sodium hydroxide solution as the circulating fluid. The effect of bottom gas flowrate and snorkel diameter in this case was also evaluated. Bottom gas injection practice, under the upleg, improves the circulation rate. Increasing the circulation rate by bottom injection leads to an increased degassing rate. However, degasification efficiency does not remain at the same level. The circulation and degasification rates can be improved by an increase in diameter of the downleg snorkel. The relative gain in degasification seems to be higher at the higher flowrate range. The results have been translated to a prototype, to optimise the process.

Keywords: RH degasser, Decarburisation, Physical modelling

Introduction

The RH (Ruhrstahl–Heraeus) degassing process is widely used for the secondary refining of steel, including decarburisation, the removal of nitrogen, hydrogen, inclusions, etc., and alloy additions and so on can be can be made with efficiency depending upon the specification of the final product. During RH treatment, molten steel is circulated between the vacuum vessel and the ladle, and as such, the circulation rate as well as stirring effects have an important influence on the rate of degassing, in addition to the degree of vacuum. These in turn are dependent on the gas injection rate through the nozzles, depth of injection, inside diameter, morphology, length and number of snorkels, amount of hot metal in the ladle and the temperature. As well as these parameters, operating problems such as nozzle blockage have a significant influence on the circulation rate. Several studies have highlighted the effects of various parameters on the circulation rate and mixing time, such as snorkel diameter, argon gas flowrate, etc., using tracers such as potassium chloride.[1–3] Circulation rates have also been measured using radioisotopes.[4] The general conclusions of these investigations are that the circulation rate increases with increasing inner diameter of the upleg and gas flowrate,[5] which in turn results in better degassing rates. Generally speaking, the main goal is to reduce the tap–tap time in order to synchronise better the degassing operation and casting. Models, both macroscopic and microscopic, are available in the literature differing in detail but generally in agreement with the idea that refining is faster when the circulation rates are greater. In one of the macroscopic models[6] the rate of decarburisation is given by

$$\ln \frac{\%C_f}{\%C_i} = -K_C t \tag{1}$$

where $\%C_f$ and $\%C_i$ represent the final and initial carbon concentrations, respectively, t is the time (min) and K_C is a kinetic parameter relating to decarburisation (min^{-1}). On the other hand, K_C would be dependent on the circulation rate according to

$$K_C = \frac{Q}{\rho V} \frac{q}{(Q/\rho)+q} \tag{2}$$

[1]Department of Metallurgical Engineering and Materials, Universidade Federal de Minas Gerais (UFMG), Belo Horizonte, Brazil
[2]Department of Metallurgical and Materials Engineering, Universidade Federal de Ouro Preto (UFOP), Ouro Preto, Brazil
[3]Companhia Siderúrgica de Tubarão (CST), Vitória, Brazil

*Corresponding author, email seshadri@demet.ufmg.br

Published by Maney on behalf of the Institute
Received 14 December 2004; accepted 15 August 2005
DOI 10.1179/174328106X80019

where Q is the circulation rate (kg min^{-1}), V is the volume of steel in the ladle (m^3), ρ is the steel specific gravity (kg m^{-3}) and q is a volumetric mass transfer coefficient (m^3 min^{-1}). The last parameter is time dependent, and can be evaluated from[6]

$$q = 0{\cdot}26\, Q^{0{\cdot}64} A_v \%C \tag{3}$$

where A_v is the vacuum chamber cross-sectional area (m^2).

Another model[7] is based on the assumption that a refining reaction such as decarburisation takes place at the surface of bubbles rising in the upleg and at the surface of droplets ejected by vigorous stirring, as well as at the surface of liquid in the vacuum chamber. The last mentioned contribution is given by

$$\frac{dC}{dt} = -\frac{F}{V} k(C - C_e) \tag{4}$$

where C and C_e represent the instantaneous and equilibrium compositions, F is the area of the effective reaction interface, V is the volume of the bath inside the vacuum chamber and k is a mass transfer coefficient. The parameter k can be evaluated from penetration theory, using the velocity of molten steel at the upleg outlet. During the integration process, this contribution must be evaluated for a time interval equal to the residence time of metal inside the chamber. As far as the shop floor is concerned, an appropriate combination between deep vacuum and high circulation rate would guarantee that the requirements for composition and productivity are met. For evaluating the residence time of the metal inside the vacuum chamber, the circulation rate is required.

In the present work, the effect of gas injection through a porous plug on circulation rates and carbon removal for the conditions of operation of the RH degassing unit of CST (Companhia Siderúrgica Tubarão, Vitória, Brazil) steel plant has been studied through physical modelling. The objective is to assess whether the circulation and degassing rates can be improved in order to shorten treatment times without compromising quality.

Methodology

The water model of the RH unit of CST was constructed (in acrylic) with a scale factor of 1:5, considering geometric and dynamic similarity criteria based on Reynolds and Froude numbers as well as proportional flows of gas and liquid in the system. These dimensional groups had been considered with success in a previous simulation carried out with the RH degassing units of two steel plants in Brazil,[7] where correlations between dimensionless groups were evaluated for the model and then translated to the industrial process. In a recent physical modelling study,[8] fluid flow and mixing characteristics as well as influence of bottom gas injection and nozzle blockage of the RH degassing unit of the CST steel plant were investigated. The water model used in the present work was practically the same as that used in the above study. Table 1 lists operational and geometric parameters of the prototype and the corresponding values obtained by applying similarity principles for the physical model.

Figure 1 illustrates the experimental setup. The vacuum vessel was equipped with two snorkels and 16 nozzles in the upleg (two levels). Air was used for injection through the nozzles. The upleg and downleg diameters were 150 mm, snorkel immersion depth was 60 mm and liquid level in the vacuum vessel 65 mm. These are basic data for standard operation. Most were varied during the experiments in order to assess their influence upon operation. The air flowrates actually used fell short of the estimated maximum air flowrates in the model, namely 600 L min^{-1} (STP). It was noted that entrapped air was drawn downwards in the downleg at flowrates above 300 L min^{-1} (STP).

Circulation was studied using potassium chloride solution as tracer and conductivity measurements to evaluate tracer concentration with time. Air was injected through the nozzles as well as the bottom of the ladle (under the upleg). For each operational condition simulated, changes in composition were measured in the downleg by means of a conductivity meter. The

Table 1 Parameters of industrial RH (Ruhrstahl–Heraeus) degasser unit and physical model

Parameters		Prototype	Model
General	Vacuum level, mbar	0·67	984
	Working temperature, °C	1560	25
	Fluid	Steel	Water
	Liquid specific gravity, kg m^{-3}	7000	1000
Vessel	Internal diameter, mm	2245	449
	Length, mm	7600	65*
Snorkels	Length, mm	1820	364
	Internal diameter, mm	750	150
	Distance between longitudinal axes, mm	1540	165
	Depth of immersion, mm	450	90
Gas injection system	Gas	Argon	Air
	Flowrate, NL min^{-1}	2500	600
	Gas specific gravity, kg m^{-3}	0·13	1·123
	Distance between injection levels, mm	175	35
	Nozzle diameter, mm	8	1·6
Ladle	Volume of liquid, m^3	45	0·360
	Upper internal diameter, mm	4200	840
	Lower internal diameter, mm	3650	730
	Height, mm	4420	880
	Liquid level, mm	3650	730
	Freeboard, mm	600	120

*Height necessary for lifting water level depending on application of vacuum in vacuum chamber.

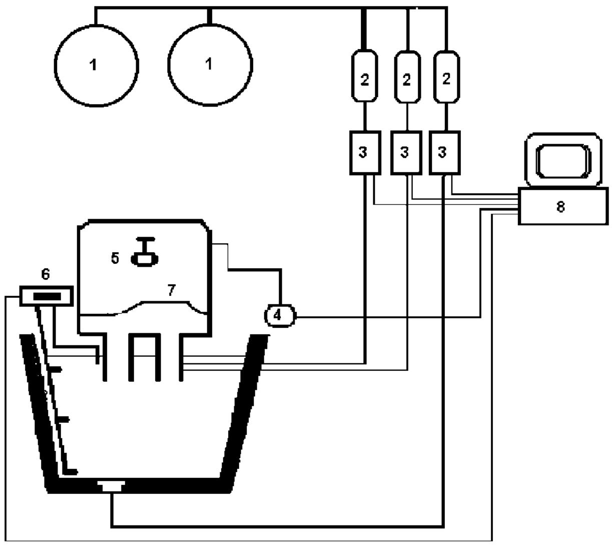

1: air compressor; 2: pressure regulator; 3: mass flowmeter; 4: pressure transducer; 5: to vacuum pump; 6: conductivity meter; 7: injection point; 8: PC and A/D board

1 Experimental setup for cold model studies of decarburisation in RH (Ruhrstahl–Heraeus) degassing unit of CST (Companhia Siderúrgica Tubarão, Vitória, Brazil) steel plant

conductivities as well as gas flowrates were continuously registered with an analog/digital PC board. With tracer injection at the vacuum chamber, in pulse mode, concentration versus time curves were evaluated (Fig. 2). A mass conservation balance shows that the circulation time can be evaluated as the ratio $A/\Delta C$, where A is the area under the first peak of the curve and ΔC is the increment of tracer concentration after stabilisation.

The rate of decarburisation was also studied using the same physical model. Simulation of decarburisation was done by evaluating CO_2 adsorption–desorption using sodium hydroxide solution, 0·02M, as circulating fluid.[9] The solution was first saturated by CO_2 blowing in order to achieve a pH ~6. Injection of air through the nozzles of the upleg caused desorption of CO_2 and this led to a change in pH to a value ~7. This technique relies on the hypothesis that in caustic solutions, equilibrium between species $H_2O(l)$, H^+, OH^-, $H_2CO_3(aq)$, HCO_3^-, CO_3^{2-}, $CO_2(aq)$ and Na^+ can be achieved quickly, when the solution contacts a gaseous phase containing $CO_2(g)$ and/or air. As shown in Fig. 3, for a limited range of pH (in this case 6–7), the reaction is predominantly desorption–adsorption ($CO_2(g)=CO_2(aq)$). Changes in the pH value are then related to $CO_2(aq)$ concentration. Thus, a macroscopic kinetics model can be proposed, assuming perfect mixing. Accordingly

$$\ln(C/C_0) = -[K(A/V)]t \tag{5}$$

where C is the concentration of CO_2 (mol L^{-1}), C_0 is the initial concentration of CO_2 (mol L^{-1}), A is the liquid/gas interfacial area (m^2), V is the volume of liquid (L), t is the time (s) and K is the mass transfer coefficient at the gas/liquid interface. From the slope of a $\log C$ versus t plot, the lumped kinetic parameter $KA/(2{\cdot}303V)$ can be evaluated (Fig. 4).

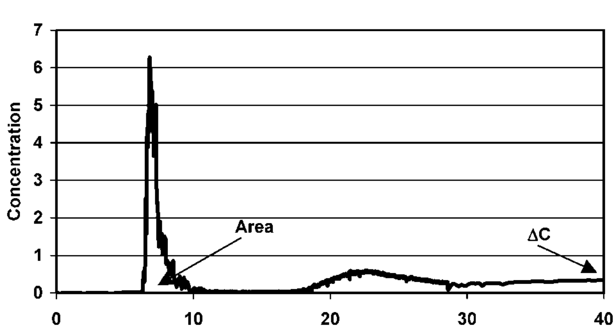

2 Typical concentration–time curve for calculation of circulation rate: (A: area under first peak, ΔC: difference between final concentration and initial concentration of tracer)

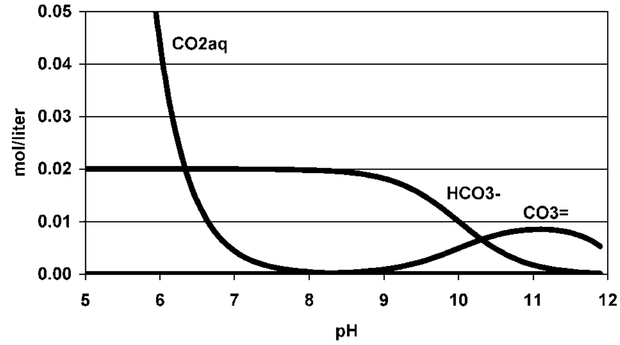

3 Equilibria between species in sodium hydroxide solution ([NaOH]=0·02 M) and gas phase containing CO_2

Results and discussion

The ladle was equipped with a porous plug for bottom gas injection in experiments with auxiliary injection. In actual plant practice, this is mainly meant for enhanced inclusion flotation. Theoretical analysis as well as plant trials have suggested that the gas flowrate combined with a vacuum is sufficient for effective degasification reactions. However, increasing the gas flowrate increases the availability of nucleation sites as well as the circulation rate, and this is generally beneficial. Physical limitation exists with regard to the plug location, since direct impingement from the steel stream is to be avoided. Hence, some plug–snorkel orientations are not feasible, even if desired. Circulation rates have been determined for various injection rates through the porous plug located at the bottom of the ladle for given gas injection using the nozzles. The experimental results show that the practice of gas injection from the bottom

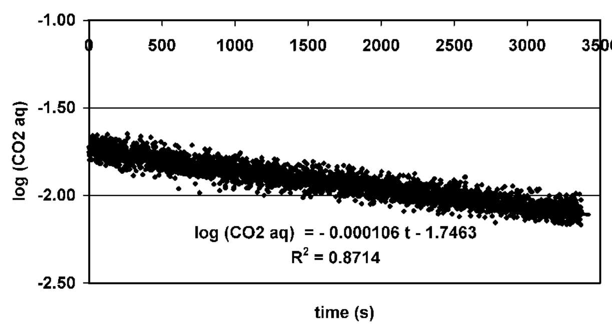

4 Kinetics of CO_2 desorption from NaOH solution

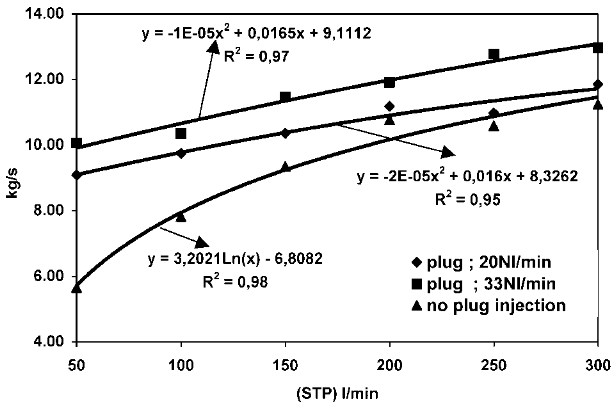

5 **Effect of gas flowrate and bottom injection (porous plug) on circulation rate as determined for water model: *x* axis relates to gas injected through upleg only**

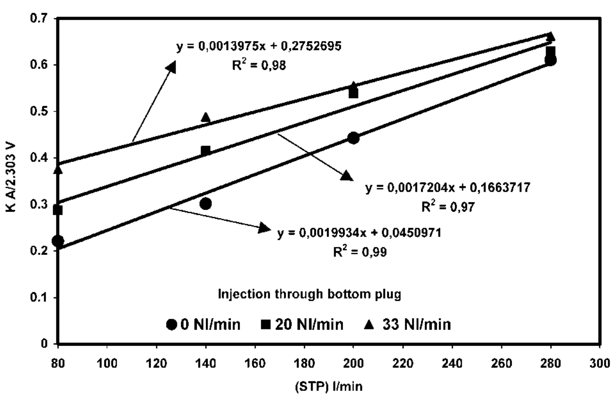

6 **Lumped kinetic parameter *KA*/(2·303*V*) (where *K* is mass transfer coefficient, *A* is liquid/gas interfacial area, *V* is volume of liquid) versus gas flowrate with and without gas injection through porous plug: *x* axis is for gas injection through upleg only**

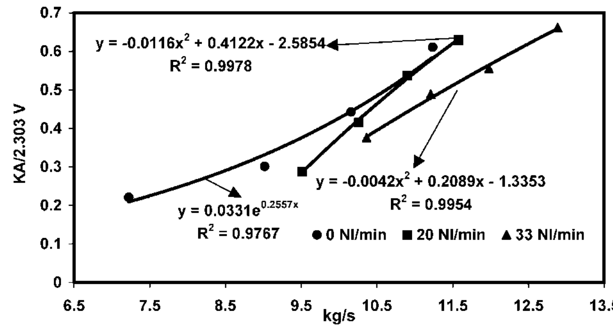

7 **Lumped kinetic parameter versus circulation rate upon degassing for given rates of gas injection through porous plug as determined for water model**

through the porous plug improves the circulation rate of the steel (Fig. 5).

Figure 6 shows experimental results for the adsorption–desorption kinetics. It can be seen that increased degassing rates result from increasing injection rate through the nozzles as well as rate of gas injection through the porous plug, as these factors also increase the circulation rate. To confirm whether injection from the bottom can replace injection through the nozzles as far as degassing is concerned, more experiments are necessary. It should be remembered that degassing is also enhanced by a higher vacuum. Data for circulation with and without auxiliary gas injection, gas flowrate and apparent degasification parameters have been combined in order to highlight the influence of circulation rate. The main objective is to assess whether the same circulation rate will guarantee the same degasification. Data from Fig. 5 (circulation rate *v*. gas flowrate) can be combined with data from Fig. 6 (lumped kinetic parameter *v*. gas flowrate) to generate Fig. 7 (lumped kinetic parameter *v*. circulation rate). As shown in Fig. 7, the degasification level is not the same even if the circulation rate is kept constant for different combinations of gas injection through the porous plug and upleg. For example, a circulation rate of 10·5 kg s^{-1} can be achieved by different gas flowrates through the upleg nozzle only, or with some auxiliary gas (plug) injection (Fig. 5). For this circulation rate, and considering the working formulae from Fig. 7, the comparison given in Table 2 can be made.

Newer degasser facilities are designed for higher circulation rates. For example, the degassing unit at CST is capable of 180 t min^{-1} (3000 kg s^{-1}). This acknowledges the positive effect of steel circulation but raises severe refractory erosion problems. Even so, new approaches towards higher refining rates are always under consideration. One consists of keeping the up snorkel geometry the same and enlarging the down snorkel diameter. To compare the influence of the down snorkel diameter on circulation and degasification, the standard operational parameters including depth of immersion of the legs and liquid levels in the ladle and in the vacuum vessel were maintained the same. The diameter of the upleg was kept constant at 145 mm (dimension in the model), and experiments were carried out for two diameters of the downleg, 145 or 180 mm (dimensions in the model). The methodology of determination of circulation time and the kinetic constant of degasification were the same as described above.

Figure 8 presents data for circulation as a function of gas flowrate (model) for the two diameters of downleg, and includes the regression curves. As expected, the larger is the diameter the larger is the circulation rate. The average relative gain (ARG) estimated from the regression ranges between 7 and 10% (Table 3).

Similarly, Fig. 9 shows values of the kinetic constant of degasification as a function of gas flowrate (in the model) for the two diameters of downleg. The largest values of constant are obtained for the largest diameter

Table 2 Comparison of degasification rates* with and without auxiliary injection

Condition	Working formula, Fig. 7	*KA*/(2·303*V*)
No auxiliary	$0{\cdot}0331\exp(0{\cdot}2557Q)$	0·4851
Auxiliary 20 L min^{-1}	$-0{\cdot}0116Q^2+0{\cdot}4122Q-2{\cdot}5854$	0·4638
Auxiliary 33 L min^{-1}	$-0{\cdot}0042Q^2+0{\cdot}2089Q-1{\cdot}3353$	0·3951

**Q* is circulation rate, *KA*/(2·303*V*) is lumped kinetic parameter.

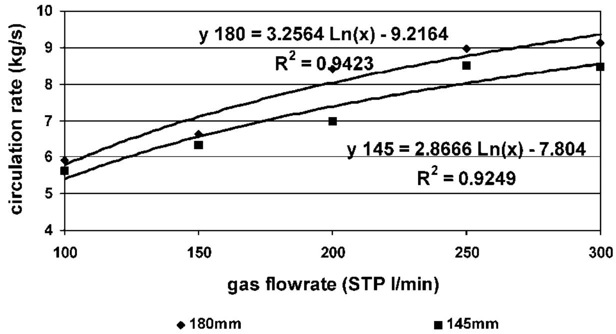

8 Liquid circulation rate versus gas flowrate for two downleg diameters 180 and 145 mm: upleg diameter is kept at 145 mm

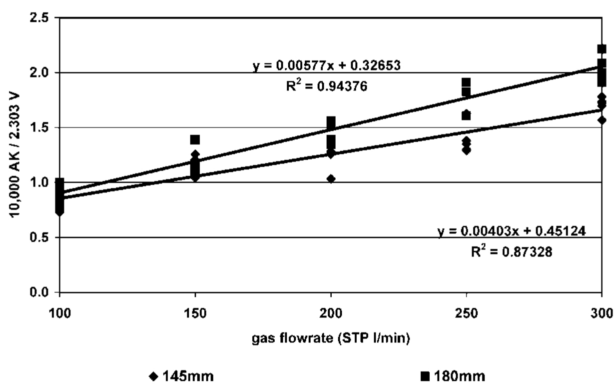

9 Lumped kinetic parameter versus gas flowrate for two downleg diameters 180 and 145 mm: upleg diameter is kept at 145 mm

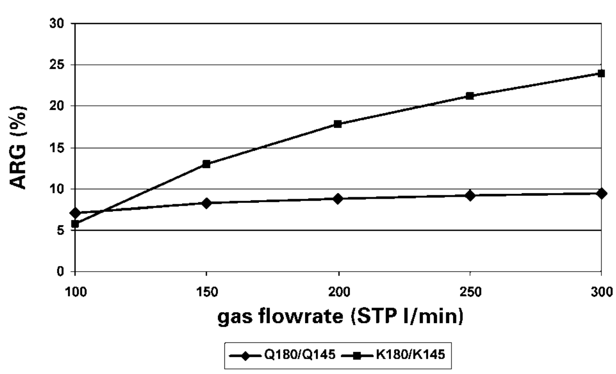

10 Circulation average relative gain (ARG) ($Q$180/$Q$145) and degasification ARG ($K$180/$K$145) as function of gas flowrate for two downleg diameters 180 and 145 mm

and ARG (estimated from the regression equations) ranges between 5 and 23% (Table 4).

Figure 10 summarises the results, presenting the ratio of circulation rates for 180 mm snorkel/145 mm snorkel as a function of gas flowrate, as well as the ratio of kinetic parameters for both cases. Improvement in degasification seems to be more important than improvement in circulation, since the gain of degasification is greater than the gain of circulation, mainly at the high flowrate range. Thus, if a reliable refractory component with high erosion resistance is available, enlargement of the downleg cross-sectional area, keeping the same vessel geometry, would result in increased circulation rate and degasification rate without deleteriously affecting the vessel service life.

Table 3 Average relative gain (ARG) of circulation rate for 180 mm dia. snorkel relative to 145 mm dia. snorkel for various flowrates of inert gas

Flow, NL min^{-1}	ARG, %
100	7·09
150	8·24
200	8·84
250	9·22
300	9·49

Table 4 Average relative gain (ARG) for degasification rate: 180 mm *v.* 145 mm

Flow, NL min^{-1}	ARG, %
100	5·77
150	12·91
200	17·76
250	21·27
300	23·93

Conclusions

1. A physical model simulating the RH degassing practice at CST (Companhia Siderúrgica Tubarão, Vitória, Brazil) is satisfactory in verifying results of earlier investigations in the field, such as an increase of circulation rate with an increasing gas injection rate in the upleg.

2. The bottom gas injection practice, under the upleg, improves circulation rates. This effect is more significant for a low snorkel gas flowrate. Increasing the circulation rate by bottom injection is followed by an increase in the degassing rate. However, degasification efficiency does not remain at the same level. In this aspect, auxiliary injection is no substitute for upleg injection.

3. Both circulation and degasification rates can be improved by increasing the diameter of the downleg snorkel. The relative gain in degasification seems to be higher at higher flowrate ranges.

Acknowledgements

The authors wish to thank Companhia Siderúrgica Tubarão, Vitória, Brazil (CST), for funding this research, and CNPQ Brazil for providing research assistantships.

References

1. S. Inoue, Y. Furuno, T. Usui and S. Miyahara: *ISIJ Int.*, 1992, **32**, 120–125.
2. V. Seshadri and S. L. S. Costa: *Trans. Iron Steel Inst. Jpn*, 1986, **26**, 133–138.
3. H. Watanabe, K. Asano and T. Saeki: *Trans. Iron Steel Inst. Jpn*, 1969, **9**, 487–501.
4. T. Kuwabara, K. Umezawa, K. Mori and H. Watanabe: *Trans. Iron Steel Inst. Jpn*, 1988, **28**, 305–314.
5. S. L. S. Costa, J. L. R. Pimenta, H. N. Barros and V. Seshadri: *Metal. ABM*, 1986, **42**, 253–256.
6. R. J. Fruehan (ed.): 'The making, shaping and treating of steel', 11th edn, 'Steelmaking and refining' Vol., 696–697; 1998, Pittsburgh, PA, AISE Steel Foundation.
7. J. H Wei and N. W. Yu: *ISS Steelmaking Conf. Proc.*, 2002, **85**, 687–704.
8. C. A. Silva, I. A. Silva, V. Seshadri, E. M. C. Martins, C. A. Perim and G. A. Vargas Filho: *Ironmaking Steelmaking*, 2004, **31**, 37–41.
9. G. A. Irons, D. Guo and D. Anghelina: *ISS Steelmaking Conf. Proc.*, 2001, **84**, 941–951.